Environmental Science: Atmospheres

ROYAL SOCIETY OF CHEMISTRY

PAPER

View Article Online
View Journal | View Issue

Cite this: *Environ. Sci.: Atmos.*, 2026, **6**, 515

Oxidative potential of fine particle emissions of a residential wood-fired boiler

Marie Khedari, *[ab] Audrey Villot,[a] Joulanda Taha,[a] Olli Sippula,[b] Pasi Jalava[b] and Yves Andres[a]

Biomass combustion emits significant amounts of airborne particles, which have been recognized for their environmental and health risks for decades. Oxidative potential (OP) is one of the health-relevant metrics introduced frequently to assess airborne particles in recent years. This study investigates the OP offresh particulate matter with an equivalent aerodynamic diameter of less than or equal to 1 μm (PM_1) emitted from a residential biomass boiler (15 kW). Four biomasses, including hardwood chips, softwood chips, hardwood pellets, and softwood pellets, were studied. The sampled PM_1 was characterized for its physicochemical properties and analyzed with two OP assays, including ascorbic acid (AA) and dithiothreitol (DTT). The average intrinsic OP_m^{AA} ranged from 0.005 to 0.018 nmol min^{-1} μg^{-1}, and volume-normalized OP_v^{AA} was 304.0 to 583.5 nmol min^{-1} m^{-3}. For DTT assay, the range was 0.0002 to 0.004 nmol min^{-1} μg^{-1} for OP_m^{DTT}, and 20.9 to 68.7 nmol min^{-1} m^{-3} for OP_v^{DTT}. More importantly, biomass types with high combustion-emitted PM emissions did not necessarily exhibit high OP, highlighting particle chemical composition as a key determinant of OP. Significant correlations were observed between the organic carbon (OC) fraction and intrinsic OP, underscoring the role of particulate organic components in driving OP from biomass combustion emissions. These findings emphasize the importance of multi-assay OP approaches and provide critical insight into the contribution of combustion emissions from different biomass fuels to ambient air.

Received 29th December 2025
Accepted 4th March 2026

DOI: 10.1039/d5ea00177c

rsc.li/esatmospheres

Environmental significance

Current standard measurement methods focus exclusively on particle mass concentration without incorporating health-relevant metrics for biomass combustion emissions. The recent EU air quality directive (2024/2881) recommends measuring oxidative potential (OP) at supersites for ambient air monitoring. Understanding the relationship between OP and primary emission sources, particularly biomass combustion, is therefore essential. This study showed that biomass combustion with high PM mass concentrations did not necessarily have high OP. More importantly, a significant correlation was found between the organic carbon (OC) ratio and OP values. Given the high carbonaceous compound emissions from biomass combustion, the particulate organic fraction is an important contribution in understanding the role of emission sources in atmospheric pollutants and OP.

1 Introduction

Biomass combustion has long been recognized as a significant source of airborne particles, contributing to both environmental and health concerns.[1–3] With an emerging trend in studying health effects related to biomass combustion particles,[4] attention has been increased toward determining the oxidative potential (OP) of these particles globally.[5–9] OP is defined as the ability of airborne particles to generate reactive oxygen species (ROS).[10] OP can be considered as a proxy of oxidative stress, a critical mechanism underlying the adverse health effects of particle exposure.[11] Growing literature has found the association of oxidative stress with several adverse health effects, such as acute respiratory distress syndrome (ARDS), chronic obstructive pulmonary disease (COPD), asthma, metabolic dysfunction, cancer, and cardiovascular diseases.[12–16] Oxidative stress is caused by the imbalance of free radical generation[17] such as excessive reactive oxygen species (ROS) production, and a weakening of antioxidant defense in cells and tissues.[18,19] For instance, a depletion of reduced glutathione (GSH) in exchange for a rise in oxidized glutathione (GSSG) leads to a decreased ratio of intracellular GSH/GSSG.[20] One of the possible causes of oxidative stress is the capacity of particles to induce oxidation while in contact with the cells. Thus, OP is recognized as an estimate of the capacity of PM in inducing oxidizing reactions at the cellular and molecular level.[13]

[a]*Department of Energy Systems and Environment, IMT Atlantique, GEPEA, UMR CNRS 6144, F-44307 Nantes, France. E-mail: marie.khedari@imt-atlantique.fr; marie.khedari@uef.fi*

[b]*Department of Environmental and Biological Sciences, University of Eastern Finland, Yliopistonranta 1, P.O. Box 1627, FI-70210 Kuopio, Finland*

According to the EU Directive (2024/2881), OP of PM is currently included as an emerging concern to be measured in supersites along with ultrafine particles, black carbon, elemental carbon and ammonia.[21] OP is suggested to be one of the highly relevant indicators of PM toxicity and has been widely applied in PM assessment research.[22,23] As OP involves chemical compounds and redox activity of PM, it is considered more relevant for assessing PM and its potential health-related effects compared to particle mass concentrations alone.[24–26] Various assays are available for assessing OP of PM, acellular assays are usually applied due to their practicality and cost-effectiveness.[27] In this study, ascorbic acid (AA) and dithiothreitol (DTT) assays were implemented. AA has been found to react with redox-active transition metals, including Fe and Cu.[28–31] DTT has been observed to react with transition metals, organic compounds, quinones, and secondary organic aerosols.[32–35] It has been suggested that the variations in OP^{AA} and OP^{DTT} were attributed to antagonistic metal–organic and metal–metal interactions as well.[36] Consequently, the combined use of both assays is expected to capture the major range of oxidative-active components in PM from biomass combustion.

As wood species and their compositions vary across regions, the use of different solid biomass types leads to different emission profiles.[37,38] Specifically for particulate emissions, the current requirement on residential wood burning in the EU is 40 mg m^{-3} for automatically stoked boilers.[39] However, there is growing debate about whether mass concentration is sufficient for categorizing emissions. Since modern wood-burning appliances tend to produce less mass compared to older technologies, the emitted particles were observed to have smaller sizes.[40,41] The emissions of residential wood combustion were found to contribute to the presence of particles down to 20 nm.[42] As smaller size particles such as PM_1 (aerodynamic diameter $\leq$ 1 μm) and ultrafine particles (aerodynamic diameter $\leq$ 0.1 μm) can penetrate deeper and translocate within the human body, they retain longer and can cause more pulmonary inflammation.[43] Recent research has surged in the PM_1 study to define its health impacts, especially respiratory diseases.[44]

Although the OP metric has been increasingly applied to assess PM emissions, critical methodological aspects remain unresolved, including which PM size fraction should be measured and how samples should be collected and processed. The current OP application has remained largely focused on ambient air measurements, for which the analyzed PM consists of complex mixtures of fresh and aged aerosols from various sources.[22,32,35,45] Existing OP studies report highly variable results, reflecting differences in emission source characteristics, PM compositions, assay sensitivity, and dominant drivers of different OP assays.[31,36] Previous OP investigations on biomass combustion emissions have mostly examined specific scenarios, such as heavily impacted ambient particles[8,46] or emissions from cooking and residential stoves,[6,47] often under conditions that may include air mixing and secondary aerosol formation. In contrast, the OP of primary combustion-emitted PM from different wood-based biomass fuels used in residential heating remains scarcely addressed.

To address this gap, the objectives of this study are to investigate the OP^{AA} and OP^{DTT} of the primary emitted PM_1 from biomass combustion, and to find potential associations with biomass and emitted particle characteristics. Four different commonly used biomass fuels were studied to reveal the differences in the emissions and OP. The biomasses were characterized for their elemental compositions and burned in a 15 kW residential heating boiler. The emitted PM_1 of each biomass combustion was measured and collected on quartz filters, which were then analyzed with a scanning electron microscope and energy-dispersive X-ray spectroscopy (SEM-EDX), and a thermal-optical carbon analyzer (Organic carbon - Elemental carbon). The sampled PM_1 was extracted for inductively coupled plasma mass spectrometer (ICP-MS) analysis, and OP^{AA}, and OP^{DTT} assessment. By incorporating multi-analytical perspectives, this study contributes to a better understanding of the relationships between biomass fuel type, combustion-emitted PM composition, and their potential implications for combustion-related health effects.

2 Materials and methods

2.1. Biomass characterization

Four biomass fuels used in this study were hardwood chips, softwood chips, hardwood pellets, and softwood pellets. All biomasses were originated from the Pays-de-la-Loire region in France. The biomasses were mostly a mixture of local wood types, except for hardwood pellets which consisted of only chestnut wood, an industrial waste product.

2.1.1. Ultimate analysis (CHNS-O). The ultimate analysis was implemented to determine chemical elements, including C, H, N, S, and O, by mass of the samples. All biomasses were finely ground into powder by using ball milling (Mixer Mill MM400, Retsch), and oven-dried before performing the ultimate analysis. The triplicate of 1 mg of biomass samples was tested in a CHNS-O elemental analyzer (Flash EA1112, Thermo Finnigan).

2.1.2. Ash content and inorganic elemental analysis. All biomass samples were ground and dried for at least 24 hours at 105 °C. The triplicate of 5 g per each biomass was placed in crucibles and taken into the muffle furnace (P330, Nabertherm). The temperature was raised to 550 °C and kept for 5 hours, with the heating rate of 10 °C per min. According to EN ISO 18122, ash determination at 550 °C allows the retention of carbonates. After combustion, the samples were left to cool down in a desiccator then weighed. The ash content is expressed as the percentage of ash weight over the oven-dried sample.

To determine the inorganic elements of the ashes for each biomass, the X-ray Fluorescence Spectrometry testing technique was used. The ash previously produced was inserted into the X-ray spectrometer (EDX-800HS, SHIMADZU). The principle is that X-rays irradiate the samples. Then, the elements in the samples will emit fluorescent X-ray radiation, which can be measured and therefore allow us to characterize them.[48]

2.1.3. Proximate analysis. We performed proximate analysis with thermogravimetric analysis (TGA) to determine moisture content (MC) following ASTM D4442-20 temperature

guidelines, volatile matter (VM), and fixed carbon (FC) of the tested biomasses. TGA is a measurement technique, which measures the mass loss of a material or sample through different temperatures.[49] In this study, thermal degradation of biomasses was analyzed by using a thermogravimetric analyzer (SETSYS Evolution, SETARAM). A duplicate analysis was performed for each sample using 15 to 20 mg of finely ground biomass. The analysis chamber gradually increased the temperature, where different biomass constituents were decomposed. For proximate analysis, the temperature first increased from 25 to 105 °C with a step of 20 min to evaporate the water content in the biomass. Then, the chamber was heated to 950 °C with a heating rate of 10 °C min^{-1} and a nitrogen flow rate of 20 ml min^{-1} to ensure the decomposition of volatile matter.[50] The samples were then cooled to 550 °C and maintained under oxygen conditions for ash determination. The mass losses at different temperature intervals correspond to different components of the biomass. Fixed carbon was then calculated by applying eqn (1).

$$FC = 1 - (MC + VM + AC) \quad (1)$$

2.2. Particle sampling and analysis

2.2.1. Particle sampling and measurement. This study used an HKRST 10N FSK 500 biomass boiler (REKA) with a nominal power of 14.9 kW installed at the Energy Systems and Environment Department (DSEE), IMT Atlantique, Nantes, France. At 1 m from the combustion chamber, we implemented the high-temperature sampling (180 °C) following ADEME (the French agency for ecological transition) recommendations based on the DIN+ standard[51] to prevent condensation of semi-volatile compounds. The boiler output power was maintained at 15 ± 3 kW, and the temperature difference between the flow and return water was approximately 10 °C during sampling, ensuring stable operating conditions. During the campaigns, biomass consumption rates ranged from 3 to 4 kg h^{-1} for all tested biomasses. The boiler operation was consistent with the manufacturer's technical specifications provided in the supplementary material (Table S1).

Particle sampling was conducted using quartz filters (Whatman™) with a PM_{10} impactor (DEKATI®) with three-stages for size-segregated sampling of PM_{10}, $PM_{2.5}$, and PM_1 fractions. Prior to the sampling campaign, all quartz filters were pre-baked at 500 °C for 5 hours to eliminate organic contaminants. The filters were then conditioned for up to 24 hours in the laboratory (20–21 °C, 40 ± 5% RH) before weighing. PM_1 was collected on 47 mm quartz filters positioned at the impactor's final stage. Exhaust gas was drawn through a temperature-controlled heating line at 180 °C with a flow rate of 10 lpm, then passed through the impactor, which was maintained at 180 °C using a heating jacket during 10 minute sampling periods.

Particle number size distributions were measured by using an electrical low-pressure impactor (ELPI, DEKATI®) with aluminum substrates and a 47 mm quartz filter at the filter stage. ELPI measures particles with an aerodynamic diameter size range of 7 nm to 10 μm. The operating principle of ELPI is based on the electrical detection of charged particles.[52] When particles enter ELPI, they are initially electrically charged. Then, the particles are classified in different low-pressure impactor stages based on their inertia and size. Upon impaction on the collection stages, the particles lose their charge, which is detected by electrometers connected to each stage. The measured current profile is converted into a particle number size distribution in real-time. In this study, a double diluter setup (DEKATI®) was used prior to ELPI to adjust a suitable particle concentration for the ELPI. The dilution air was first filtered and dried, then heated to 180 °C before entering the mixing chamber to be consistent with the drawn flue gas. The dilution ratio at a pressure of 1013 mbar is 8.38. The measurement was realized by drawing the gas through ELPI at a constant flow rate of 10 lpm.

Fig. 1 illustrates the simplified particle sampling and measurement system. For each biomass type, duplicate particle samplings were performed after the boiler achieved stable operating conditions (15 ± 3 kW). After sampling, the quartz filters were maintained at −20 °C throughout storage and transportation prior to physicochemical and oxidative potential analyses. The PM emissions in this study were expressed in dry flue gas basis at 10% O_2 and standard conditions (0 °C and 1013 mbar) to align with the Commission Regulation (EU) 2015/1189.[39]

2.2.2. PM_1 physicochemical characterization. The sampled particles were analyzed using a field-emission scanning electron microscope with energy-dispersive X-ray spectroscopy (SEM-EDX, JSM-7600F, JEOL Ltd.). The microscope has an accelerating voltage of 0.1 kV to 30 kV, eucentric specimen stage, and 5-axis motor control allowing stable and accurate tilting during observation. The magnification ranges from 25 to 100 000 on the image size 120 mm × 90 mm. As our samples were highly concentrated emissions, we carefully took a small amount of particles from the collected filters and placed them on the probe for SEM-EDX analysis. For each sample, two types of imaging were conducted. We performed the secondary electron imaging (SEI) to observe the size, morphology, shape, and agglomeration of the particles. In addition, a backscattered electron imaging (BEI) was implemented to observe the different elements in the samples.

To investigate the organic and elemental carbon (OC-EC) contents of the particles, thermal-optical carbon analysis was performed with an OC-EC laboratory analyzer (Sunset Laboratory Inc.) using the IMPROVE-A method. For each biomass fuel, a filter punch size of 0.5058 cm^2 was cut from the sampled quartz filters to be analyzed. The detection limit of the analyzer is 0.10 μg C cm^{-2}.

Elemental compositions of the particle samples were analysed using an inductively coupled plasma mass spectrometer (ICP-MS, NeXION 350D, PerkinElmer®). Nitric acid (65–68%, Trace Metal grade, Fisher Chemical™), hydrofluoric acid (40%, Trace Metal grade, Fisher Chemical™) and boric acid (4%, Suprapur grade, Merck) with MARS6 microwave digestion system (CEM Corporation, USA) at 200 °C for 15 min were used to digest the samples. Multi-element calibration standards

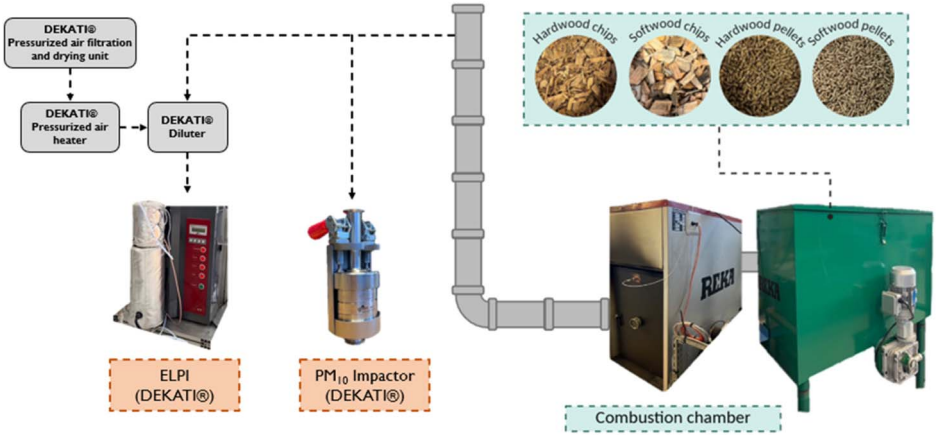

Fig. 1 Particle sampling and measurement diagram.

(TraceCERT Periodic Table mixture 1 and 2, Sigma-Aldrich) were used as calibration standards, and scandium-45 and lutetium-175 as internal standards. Blank samples and certified reference material (1648a urban particulate matter) were analyzed in the same way as the samples. Blank filters were analyzed, and the results were subtracted from the sample results. The limit of quantification is provided in the supplementary material (see Table S2). It should be noted that the particle samples analyzed with ICP-MS were extracted with HPLC-grade methanol (Fisher Chemical™) and evaporated under Nitrogen flow prior to the analysis, which is the similar method used to retrieve the collected PM_1 for oxidative potential (OP) assessment in this study.

2.3. Oxidative potential (OP) assessment

2.3.1. Ascorbic acid (AA) and dithiothreitol (DTT) assays. Despite the various uses of OP assessment, a definitive standard method for the analysis has not yet been established to the best of the authors' knowledge. We adapted the acellular OP assessment method performed on heavily impacted aerosols from residential wood burning.[8] This procedure was also done in other previous OP studies.[31,53,54] As we sampled our particles in highly concentrated conditions, the solution's concentration and volumes were adjusted and defined as follows.

Particle extraction methods vary across oxidative potential (OP) studies, with both aqueous and organic solvents commonly applied. In this study, a quarter of sampled quartz filters was cut and extracted with HPLC-grade methanol (Fisher Chemical™) and evaporated under Nitrogen flow to retrieve the collected PM_1. Methanol was selected as the extraction solvent based on previous findings showing that its polar organic properties enable efficient extraction of both hydrophilic and moderately hydrophobic organic compounds, including redox-active species relevant to OP measurements.[35,55] In particular, methanol has also been reported to recover DTT-reactive PM components more efficiently than water, while yielding comparable responses in the AA assay.[56] Additionally, methanol extraction has been recommended due to its low background contamination, cost efficiency, and its widespread and established use in PM exposure for toxicology studies.[1,57,58] Our extraction protocol, including sonication, also mechanically removes particles from the filters, and has yield in high gain of PM mass from the filters, as described in detail in Jalava *et al.*[1] Although the use of methanol may limit direct quantitative comparison with studies employing aqueous extraction, this approach provides a reproducible framework for assessing OP and supports potential future integration with cellular-based toxicological evaluations.

Following extraction, we added 0.1 M Potassium phosphate buffer (pH 7.4) to reconstitute the extracted particles and sonicated in an ultrasonic bath at 37 °C for 15 minutes. The use of potassium phosphate buffer was to mimic the human-like conditions. The extract solution was filtered on a syringe filter (0.45 μm, CA, Whatman™) and adjusted to be equally 25 ml with the buffer. The solution was divided into 2 tubes of 10 ml each for AA, and DTT assays. For AA assay, 90 μl of AA solution (10 mM in potassium phosphate buffer 0.1 M pH 7.4) was added to 10 ml of particle extract and mixed well. Then, we pipetted out 2.5 ml of the mixture into the quartz cuvette at 5, 10, 15, 20, and 40 minutes. At each time interval, we measured the absorbance with the UV-Vis spectrophotometer (UV-1800, Shimadzu) at the wavelength of 265 nm. For DTT assay, 90 μl of DTT solution (10 mM in potassium phosphate buffer 0.1 M pH 7.4) was added to the other 10 ml of particle extract and mixed well. Then, 1.5 ml of the mixture was pipetted into the semi-micro PMMA cuvette at similar time intervals of 5, 10, 15, 20, and 40 minutes. At each time point, 150 μl of DTNB (5,5′-dithiobis-(2-nitrobenzoic acid)) solution (10 mM in potassium phosphate buffer 0.1 M pH 7.4) was added and mixed before measuring the absorbance with the UV-vis spectrophotometer at the wavelength of 412 nm. Details of chemicals used in solution preparations can be found in the supplementary material (Table S3).

For each biomass fuel, we conducted the assessment on two portions of each filter. As we sampled twice per campaign, we therefore repeated the OP assessment four times for each biomass. During each measurement, a blank quartz filter was

processed with the same procedure as a controlled sample. AA, DTT, and DTNB were freshly prepared on the same day as the assessment. The assays were performed in a dark room, and the solutions were covered with aluminum foil and kept in an ice bath to avoid reacting with light and temperature before use.

2.3.2. Mass- and volume-normalized OP calculation. After the absorbance measurement, the concentration of AA and DTT can be calculated from the calibration curve ($y = mx$), where y represents the absorbance and x represents the compound concentration (see Fig. S1). A linear calibration curve described by $y = 0.0121x$ ($r^2 = 0.993$) was used for AA assay quantification over the concentration range of 0 to 300 μM. For DTT assay, a linear calibration curve described by $y = 0.0264x$ ($r^2 = 0.990$) was used over the concentration range of 0 to 90 μM. The depletion rates (nmol min^{-1}) of AA and DTT were then determined using linear regression by plotting AA or DTT concentration against time. The depletion rates were subtracted with the blank filter's depletion rate of the same assessment day to eliminate the effects of filters and artifacts.

In the OP assessment, two normalizations can be implemented to investigate the depletion kinetics. The first method is mass-normalized OP (OP_m) or intrinsic OP. OP_m (nmol min^{-1} μg^{-1}), which is obtained by normalizing the depletion rate by the mass of sampled particles introduced to the assay (μg). The second method is volume-normalized OP (OP_v). OP_v (nmol min^{-1} m^{-3}) by normalizing the depletion rate with volume of gas sampled (m^3). Eqn (2) and eqn (3) present both OP normalization methods implemented in this study.

3 Results and discussion

3.1. Biomass compositions

Table 1 presents the characteristics of four biomasses analyzed in this study. According to the results obtained by the ultimate analysis, the CHNS-O compositions showed similar characteristics among the tested biomasses. Nitrogen was detected only in hardwood pellets, approximately at the minimum limit of concentration quantification. Consequently, the amount is considered insignificant. All biomasses were in compliance with CHNS-O compositions determined in NF EN ISO 17225-2 standard for graded wood pellets, where N and S are limited to less than 1 and 0.05% dry basis, respectively. For wood chips, the CHNS-O results fell in the same range as an existing study on wood chip characteristic investigation.[59]

Ash content is one of the factors affecting PM emissions during biomass combustion.[60] The presence of elemental compositions such as K, Na, and trace metals in biomasses can influence the PM distribution and composition, as they are among the ash-forming elements.[61,62] Depending on the fuels and combustion appliances, several heavy metals, including As, Cd, Cu, Ni, Pb, Ti, and Zn, can be released within the PM from biomass combustion.[63] From all four tested biomasses, the ash contents ranged from 0.16% to 0.75% dry basis, which were all lower than 2% requirement in the NF EN ISO 17225-2 standard. In addition, the ash-forming elements were analyzed from the biomasses (see Table S4 for detailed composition results). Despite the low quantity, we observed the distinct differentiation between wood chips and wood pellets for Al and Fe. A possible cause for the presence of these elements is the

$$\mathrm{OP_m}\left(\text{nmol min}^{-1}\ \mu\text{g}^{-1}\right) = \frac{\text{Depletion rate}_{\text{sample}}\left(\text{nmol min}^{-1}\right) - \text{Depletion rate}_{\text{blank}}\left(\text{nmol min}^{-1}\right)}{\text{PM mass introduced to assay}(\mu\text{g})}$$

$$\mathrm{OP_V}\left(\text{nmol min}^{-1}\ \text{m}^{-3}\right) = \frac{\text{Depletion rate}_{\text{sample}}\left(\text{nmol min}^{-1}\right) - \text{Depletion rate}_{\text{blank}}\left(\text{nmol min}^{-1}\right)}{\text{Volume of gas sampled}(\text{m}^3)}$$

Table 1 The characterization of biomass fuels expressed in % weight on dry basis[a]

		Wood chips		Wood pellets	
	Composition	Hardwood	Softwood	Hardwood	Softwood
Ultimate analysis	C	48.6 ± 0.3	48.3 ± 0.9	47.4 ± 0.2	50.1 ± 0.1
	H	5.7 ± 0.1	5.9 ± 0.1	5.7 ± 0.1	6.0 ± 0.1
	O	40.3 ± 1.1	41.9 ± 0.6	39.8 ± 0.5	40.2 ± 0.4
	N	<LQ	<LQ	0.2	<LQ
	S	<DL	<DL	<DL	<DL
Ash content		0.75 ± 0.04	0.16 ± 0.01	0.31 ± 0.03	0.67 ± 0.02

[a] "<LQ" is below the limit of quantification (0.2%), "< DL" is below the detection limit (0.06%). Ash content refers to ash determined at 550 °C from biomass samples.

pelletizing process during wood pellet production. We found that all of our tested biomasses had lower inorganic metals compared to the same NF EN standard. The studied biomasses had Zn from 3.77 to 28.9 mg kg^{-1} dry basis, while the standard limit is at 100 mg kg^{-1} dry basis. For Cr, Pb, and Cu, none of the biomasses presented higher than 10 mg kg^{-1} dry basis, as limited in the standard requirement. In addition, we did not detect Cd, Ni, As, and Hg, which also belong to the standard limits' elements. As a result, our biomasses met the established standards for their chemical compositions.

According to the thermogravimetric analysis (TGA), we observed higher moisture content (MC) in wood chips (12.4% and 15.8% for hardwood and softwood, respectively) compared to wood pellets (6.7% and 7.5% for hardwood and softwood, respectively). Since the pelletizing process has to ensure that the final products have lower than 10% moisture content to comply with ENplus pellet quality requirements,[64] the process involves drying. This leads to lower MC observed in commercial wood pellets compared to wood chips. However, as our boiler is capable of burning solid biomass fuels with a moisture content up to 30%, the MC of all tested biomasses falls in the acceptable range. Softwood fuels were observed to have higher volatile matter (VM) compared to hardwood fuels. Prior studies also found higher VM in softwood with higher cellulosic content but lower in lignin compared to hardwood.[65,66] Nevertheless, we did not observe a significant difference among our tested biomasses. Thus, the detailed findings are presented in the supplementary material (Fig. S3).

3.2. Particulate emissions

3.2.1. Particle mass concentration. Fig. 2 illustrates the PM mass concentration from different types of biomass samples in residential heating. For all biomasses, the mass fraction of their emissions was majorly from PM_1 contribution for approximately 90% in the total mass concentrations. The average PM_1 mass concentrations in this study ranged from 17.31 to 115.51 mg m^{-3} at 0 °C, 1 atm, 10% O_2 and dry gas. Hardwood pellets were found to emit significantly less mass concentration compared to other biomass types, being the only biomass that complied with the 40 mg m^{-3} particle emissions requirement for automatically stoked boilers according to the European Commission Regulation (EU) 2015/1189.[39] Softwood pellets emitted the highest PM_1 mass concentration. A similar trend was observed for wood chips, where hardwood emitted lower PM mass concentration compared to softwood. Nevertheless, the difference was not as significant as in wood pellets. In this study, softwood biomasses were found to emit high particle concentrations compared to hardwood during combustion. According to our TGA analysis, higher moisture content (MC) and higher volatile matter (VM) (see Fig. S3) content were found in softwood, compared to hardwood fuels, which influences their combustion characteristics and may have led to higher PM emissions. However, previous studies have found no clear dependence between wood species and their emissions when the comparison is done at comparable combustion conditions.[38,67]

3.2.2. Particle number size distribution. The total particle number concentration integrated over all sizes of combustion emissions from four tested biomasses was from 2.35×10^7 to 5.25×10^7 particles cm^{-3} normalized to 0 °C, 1 atm, 10% O_2 and dry gas condition. The geometric particle number mean diameters (GMD) were 0.17, 0.12, 0.13, 0.18 μm for the emissions of hardwood chips, softwood chips, hardwood pellets, and softwood pellets, respectively. Particle number concentration modes were observed for particles with aerodynamic diameters of 0.12 μm for hardwood chips and pellets, and 0.20 μm for softwood chips and pellets. Our GMD results fall in the comparable range with previous studies in which the GMD of particles emitted from wood combustion was measured to be from 0.06 to 0.10 μm with a 20 kW burner,[68] and 0.13 to 0.19 μm with a top-feed pellet stove.[67] As shown in Fig. 3, the number concentration of particle emissions from softwood combustion is higher than from hardwood combustion. For softwood, wood pellet combustion exhibited lower number concentrations but larger in diameter compared to softwood chips, while hardwood pellet combustion exhibited higher number concentrations, but smaller particle sizes compared to hardwood chips.

3.2.3. SEM-EDX analysis of PM_1. Fig. 4 presents graphical results from SEM-EDX analysis. Secondary electron imaging (SEI) results demonstrated that PM_1 from wood chip

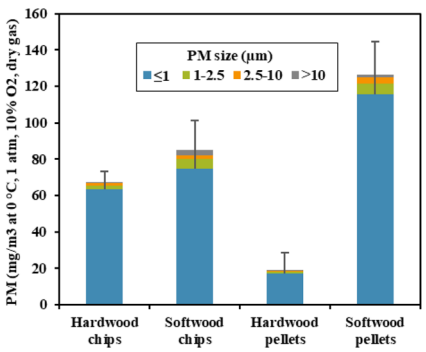

Fig. 2 PM mass concentration emitted from different biomass fuels. The bar graph shows the average with error bars representing the standard deviation of PM_1 mass concentration.

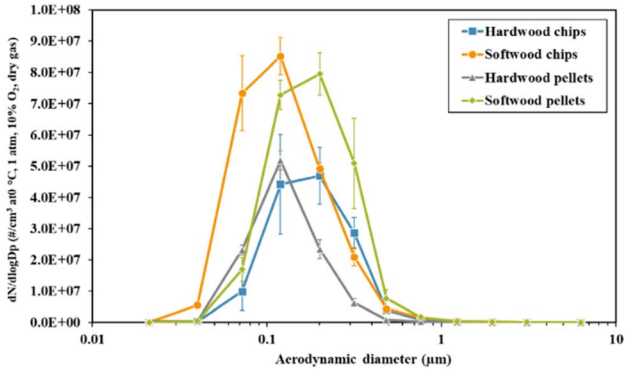

Fig. 3 Particle number size distribution from different biomass combustion. The line graph shows the average with error bars representing standard deviation.

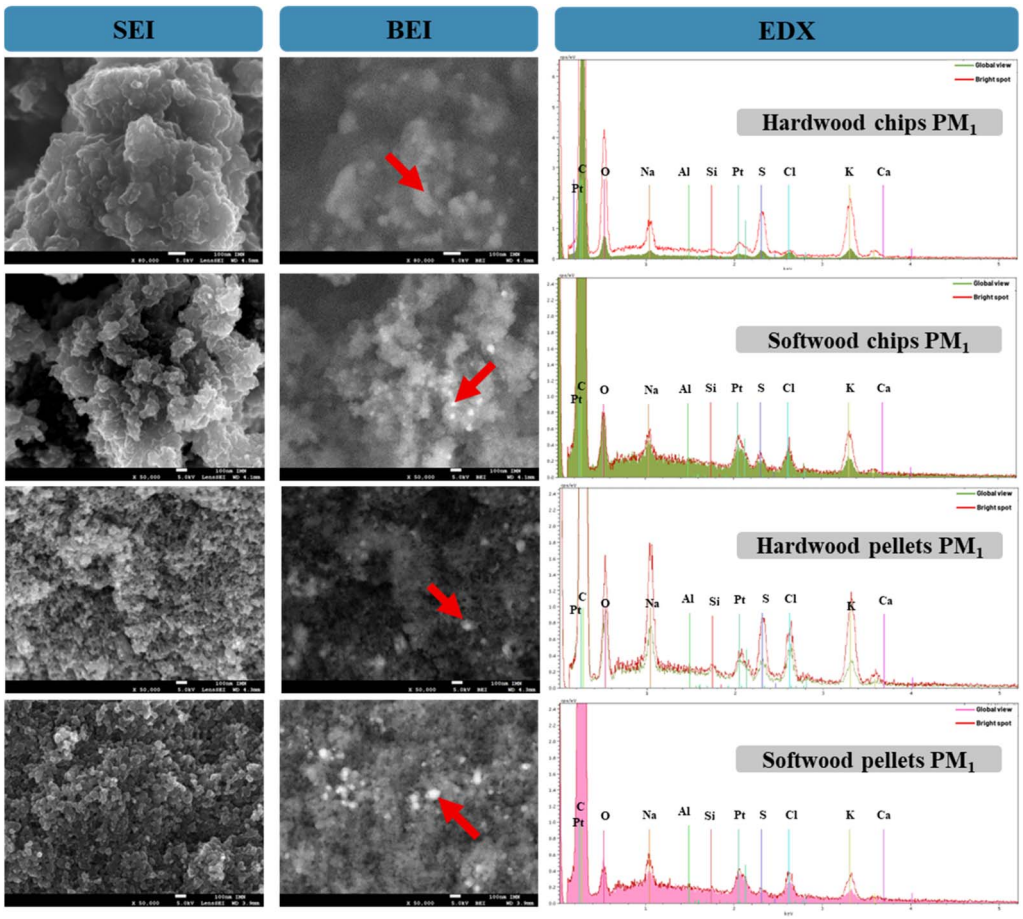

Fig. 4 SEM-EDX results of PM_1 emissions from different biomass combustion. (SEI: secondary electron imaging, BEI: Backscattered electron imaging: BEI). Note: the red arrow points to the bright spot spectrum indicated in EDX graph. The white bar below each SEM image indicates the equivalent scale of 100 nm.

combustion consisted of particles with diverse morphologies, whereas PM_1 from wood pellet combustion exhibited a soot-like agglomerate structure. These findings align with previous studies that reported biomass burning particles forming aggregated structures.[69,70] Backscattered electron imaging (BEI) allows us to demonstrate the presence of different components and elements within samples. As this imaging technique produces varying grayscale intensities, heavy elements appear as bright regions, while light elements are represented as dark or black areas. The BEI results clearly demonstrate that all PM_1 particles contain multiple elements.

To investigate the observed elemental variations within samples, we performed EDX analysis at two scales, including global view analysis for overall composition and localized analysis of bright regions. The resulting spectra were then overlaid for comparison to identify potential heavier elements responsible for the bright spots. From the global view spectrum of each sample, we identified the existence of C as a major component with others including O, Na, S, Cl, and K. Si peaks were observed in some samples, possibly originating from the quartz filter material. Pt presence was attributed to the metallization procedure performed specifically for EDX analysis. This coating process did not interfere with SEM image quality. According to the bright spot spectrum, the bright regions of all samples in BEI images corresponded mainly to areas enriched in O, Na, Cl, and K. It is important to note that the EDX analysis conducted herein allowed for qualitative elemental characterization. However, quantitative compositional analysis of PM_1 particles is limited due to the nanoscale size of the particles. Thus, the relative comparison of the spectra was implemented here.

3.2.4. OC and EC fraction of PM_1. Given the high carbon content observed in the sampled particle, OC-EC analysis was conducted to distinguish between organic and elemental carbon fractions in PM_1. The OC/EC ratios of the analyzed PM_1 samples ranged from 0.04 to 0.63. Among the tested samples, hardwood pellet particles exhibited the highest OC/EC ratio, while softwood pellet particles showed the lowest. Hardwood chips' particles were found to emit a higher OC/EC ratio of 0.21 compared to softwood chips' particles of 0.18. For all PM_1 samples, EC comprised more than half of the total carbon (TC) content, where high EC/TC was observed for biomass combustion with high PM emissions.

A large variability of OC/EC ratios of PM emissions from wood and biomass combustion has been reported in the literature, and is strongly influenced by fuel, combustion technology, and operating conditions.[71–74] For instance, OC/EC

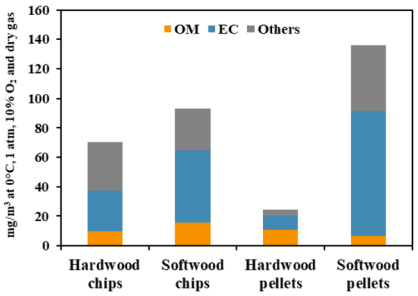

Fig. 5 Organic matter (OM), elemental carbon (EC), and other fractions of PM_1 from different biomass combustion. Note: "Others" refers to the remaining PM components not reported separately.

ratios ranging from approximately 0 to 4 have been observed for different types of woody biomass combustion in an automatic 25 kW pellet boiler,[75] while much broader ranges of OC/EC ratios (up to approximately 60) have been reported for wood burning in a residential stove.[76] OC and EC emissions from biomass combustion are generally influenced by combustion efficiency and combustion conditions, which are strongly affected by combustion temperature, residence time, oxygen availability, and mixing in the combustion chamber.[38,77,78] Lower combustion temperature is known to favor high OC/EC ratios, while higher temperatures associated with improper mixing typically promote high EC production.[73,79,80] Recently, Rinta-Kiikka *et al.* compared OC and EC emissions from a wood stove fired with wood made of different wood species.[38] They concluded that the differences in OC and EC might be due to the different physical properties of the wood, which influence combustion conditions, rather than wood species-dependent differences.[38] This could potentially explain the variations in OC/EC ratios observed in this study, indicating that combustion conditions during boiler operation may be a key contributing factor.

The particulate organic matter fraction (OM) can be estimated with the OM/OC ratio.[81] We implemented an average OM/OC ratio of 1.82, established in residential biomass and wood combustion literature[82] (see Table S5). The comparable OM/OC ratio was also observed in different wood burning literature (ranging from 1.6 to 1.8).[83] Fig. 5 showed the results of OM and other compounds. Most samples contained 5–17% OM, except for hardwood pellet emissions, which exhibited 44% OM content. PM_1 emitted from softwood chips and pellets consisted of more than 52% of EC. For hardwood chip combustion, the emitted PM_1 contained significant amounts of other compounds, which could be attributed to inorganic species.

3.2.5. Elemental compositions of PM_1. The elemental compositions of combustion-emitted PM_1 from different biomass fuels are presented in Fig. 6. The collected PM_1 samples contained several inorganic constituents, with Na and K being the most abundant elements. These alkali metals have also been reported to dominate the inorganic fraction of PM emissions from small-scale wood combustion in previous studies.[84,85] In particular, K in particle emissions has been used as a tracer for biomass combustion in source apportionment studies.[86] In the present study, the highest presence of K in the combustion-emitted PM_1 samples was observed for hardwood chips, which was also found to have the highest K content of the ash-forming elements (see Table S4). However, K release during combustion depends not only on its abundance in the fuel but also on fuel composition parameters such as the ratios of Si to K and S to Cl, which influence reactions of K in the fuel matrix and ultimately its volatilization during combustion.[87]

Interestingly, PM_1 from wood pellet combustion contained higher concentrations of metals, including heavy metals such as Cu, Cd, and Pb, compared to emissions from wood chip combustion. In addition, elevated Al and Fe concentrations were observed in PM_1 emitted from hardwood pellet combustion compared to softwood pellet combustion. These elements were also observed at higher levels among the ash-forming components of the corresponding fuels (Fig. S2). Overall, the elemental compositions of biomass combustion emissions are influenced by different factors, including the contents of ash-forming elements in the fuel and their release during combustion. Among the detected elements, Fe, Mn, Cu, Zn, and Sr have been observed to correlate with the AA assay, while K, Fe, Mn, Al, Zn, Cr, Cu, and Sr have been found to influence the DTT assay.[8,31,32,36,56,88] Despite the low quantity of inorganic contents in our sampled PM_1, the different elemental profiles for each biomass combustion emission could contribute to the variations of OP results.

3.3. Oxidative potential (OP) of PM_1

3.3.1. OP^{AA}. Fig. 7 presents the oxidative potential of AA assay for PM_1 samples. In this study, the mean intrinsic OP^{AA} or mass-normalized OP^{AA} (OP^{AA}_m) of PM_1 from hardwood pellets combustion was the highest (0.018 nmol min^{-1} μg^{-1}) compared

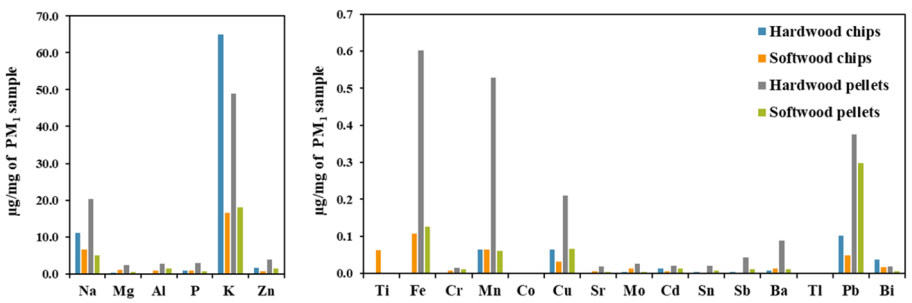

Fig. 6 Elemental compositions of PM_1 samples from different biomass combustion.

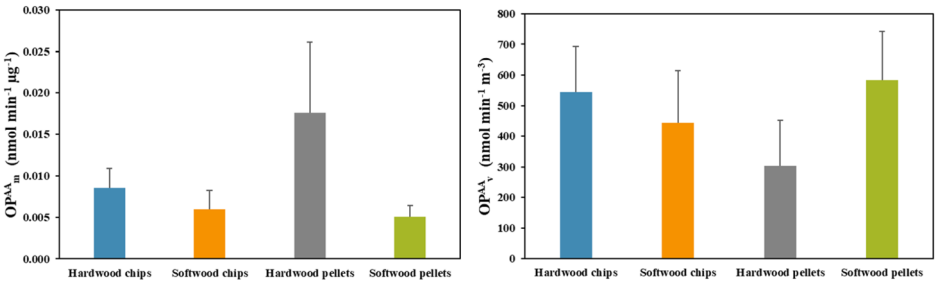

Fig. 7 OP^{AA} results of combustion-emitted PM_1 from different biomass fuels expressed in mass-normalized (nmol min^{-1} μg^{-1}) and volume-normalized (nmol min^{-1} m^{-3}). The bar graph shows the average with error bars representing the standard deviation.

to other samples. The average OP^{AA}_m for PM_1 emitted from hardwood chips, softwood chips, and softwood pellets were 0.009, 0.006, and 0.005 nmol min^{-1} μg^{-1}, respectively. The observed differences in OP results potentially resulted from varying particle compositions, notably OC-EC and inorganics, which produce different oxidative reaction mechanisms.[89] The elevated OP^{AA}_m observed for combustion-emitted PM_1 from hardwood pellets is likely associated with the high abundance of redox-active transition metals, particularly Fe and Cu, in the particle elemental composition. The AA assay is especially sensitive to such metals due to their ability to undergo redox cycling and catalyze ascorbate oxidation, with Cu(II) reported to exhibit a higher ascorbate depletion rate than Fe(III),[31] and Fe(II).[90] OP^{AA} has also been frequently linked to carbonaceous components (OC and EC) for particles collected during winter or cold seasons when biomass combustion represents a major anthropogenic emission source.[45,53] In accordance with this study, high OP^{AA}_m has been observed for combustion-emitted PM_1 with elevated OC fractions. For volume-normalized OP^{AA}, our average results range from 304.0 to 583.5 nmol min^{-1} m^{-3} for the four tested biomasses. According to the results, softwood pellet combustion emissions had the highest OP^{AA}_v values, while hardwood pellet combustion emissions showed the lowest. This pattern resulted from the exceptionally high PM_1 mass concentration of softwood pellet combustion, which surpassed other biomass samples on a volume-normalized basis. Increased particle mass directly enhances the total availability of redox-active species such as metals, which are capable of catalyzing ascorbate oxidation. Consequently, samples with moderate mass-normalized OP^{AA}_m may exhibit elevated OP^{AA}_v. However, the response may deviate from linearity due to metal solubility, redox state, and interactions with co-emitted organic components.

Although numerous studies have reported OP^{AA}, most have focused on particles collected under ambient air conditions, resulting in a wide range of OP^{AA} across different contributing-emission sources.[22,91,92] Pietrogrande *et al.* reported an average OP^{AA}_m of 0.010 nmol min^{-1} μg^{-1}, and an average OP^{AA}_v of 0.33 nmol min^{-1} m^{-3} for particles collected during autumn-winter period in Central Mediterranean, with OP^{AA} showing significant correlations with transition metals such as Fe, Cu, and carbonaceous compounds (OC, EC).[45] Consistent with these findings, Visentin *et al.* reported OP^{AA}_m values ranging from 0.007 to 0.03 nmol min^{-1} μg^{-1}, and OP^{AA}_v values between 0.2 and 0.7 nmol min^{-1} m^{-3} for particles collected during warm and cold seasons at an urban site in Bologna, Italy, where OP^{AA} was also associated with redox-active metals.[31] For particles strongly influenced by wood combustion, reported OP^{AA}_m and OP^{AA}_v values are 0.009 nmol min^{-1} μg^{-1} and 0.28 nmol min^{-1} m^{-3}, respectively.[8] Thus, the OP^{AA}_m values obtained in this study are broadly comparable to those reported in the literature for biomass combustion-influenced particles. In contrast, the OP^{AA}_v are not directly comparable, as most previous studies implemented outdoor ambient sampling with lower PM concentrations and longer sampling durations. Consequently, OP^{AA}_v values reported in ambient studies are substantially lower than those derived from highly concentrated emissions measured under stack sampling conditions in this study.

3.3.2. OP^{DTT}. Fig. 8 illustrates the OP^{DTT} of PM_1 emitted from different biomass combustion. The intrinsic OP^{DTT} of combustion-emitted PM_1 was 0.004 nmol min^{-1}.μg^{-1} for hardwood pellets, 0.0005 nmol min^{-1} μg^{-1} for hardwood chips,

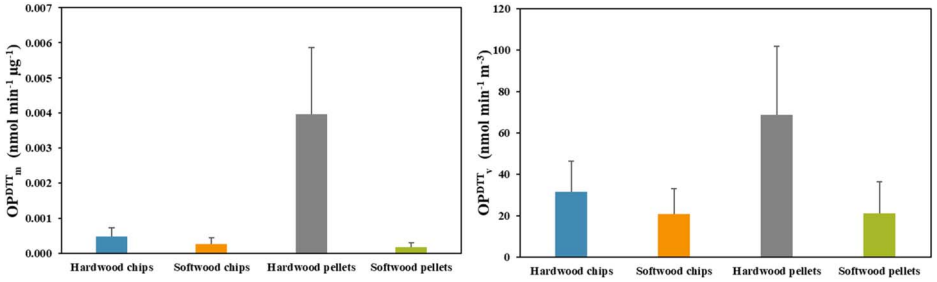

Fig. 8 OP^{DTT} results of combustion-emitted PM_1 from different biomass fuels expressed in mass-normalized (nmol min^{-1} μg^{-1}) and volume-normalized (nmol min^{-1} m^{-3}). The bar graph shows the average with error bars representing standard deviation.

0.0003 nmol min^{-1} μg^{-1} for softwood chips, and 0.0002 nmol min^{-1} μg^{-1} for softwood pellets. OP^{DTT} has been widely reported to correlate strongly with redox-active transition metals, including Cu, Mn, and Fe, in PM.[31,32,35] This behavior is also observed in the present study, where elevated OP_m^{DTT} values correspond to combustion-emitted PM characterized by higher metal content. In addition, samples exhibiting high intrinsic OP^{DTT} also showed elevated OC fractions. Carbonaceous components, organic compounds, and non-redox active metals such as K, Ca, Mg, and Zn have also been reported to influence OP^{DTT}.[35] OC, water-soluble OC, and quinone-type compounds have been frequently associated with enhanced OP^{DTT}, reflecting their strong redox activity and ability to generate ROS through redox cycling.[93,94] In particular, quinoids can act as catalysts that transport electrons from biological reducing agents to dissolved oxygen, causing a continuous production of H_2O_2 and superoxide radicals.[35]

OP^{DTT} has been widely reported to correlate with both redox-active transition metals and organic aerosol components, yet reported values for particles from biomass combustion span a broad range. Previous studies have reported OP_m^{DTT} values ranging approximately from 5 to 150 nmol min^{-1} μg^{-1} for biomass burning aerosols collected at different urban locations and sampling conditions.[46,94] In contrast, substantially lower OP_m^{DTT} values have been reported for emissions strongly influenced by combustion emissions, with values of 0.011 nmol min^{-1} μg^{-1} for heavily impacted wood combustion particles,[8] and 0.05 to 0.2 nmol min^{-1} μg^{-1} for traditional cookstove-emitted PM,[6] respectively. The relatively low OP_m^{DTT} values observed in the present study fall within the lower end of the ranges reported in the literature. Since the DTT assay responds to organic tracers and metal compounds, the stack-sampled PM, dominated by freshly emitted primary particles collected at high temperature, limits the capture of volatile and semi-volatile organic species that are known to contribute to OP.[95] Thus, the tested PM differs from particles examined in previous studies, which likely included contributions from secondary aerosols formed under atmospheric conditions. Aerosol aging represents an additional factor that may influence OP^{DTT}. Prior studies have demonstrated that oxidative aging processes can alter PM oxidative potential through ozone-driven oxidation of soot-bound PAHs, leading to the formation of quinone-like species that enhance redox activity.[35,96] Although the absence of atmospheric aging and volatile partitioning in the present study may partly explain the comparatively lower OP_m^{DTT} values, the use of stack sampling reflects standard PM emission testing protocols and provides insight into the OP of primary combustion particles. These findings further highlight the importance of particle sampling and measurement standardization.

For OP_v^{DTT}, the PM_1 of hardwood pellet combustion emissions remained highest with an average of 68.7 nmol min^{-1} m^{-3} despite its low PM mass concentration. This results from the exceptionally high intrinsic OP^{DTT} that exceeded those of particles emitted from other biomass combustions. OP_v^{DTT} was 20.9, 21.3, and 31.4 nmol min^{-1} m^{-3} for PM_1 from softwood chip, softwood pellet, and hardwood chip combustion, respectively. The interpretation of OP_v^{DTT} is inherently complex due to the non-linear interactions between particulate components and the DTT assay, particularly those involving metal ions.[31] As the assay response arises from the combined redox activity of multiple PM constituents introduced to the reaction, synergistic and antagonistic interactions among metals and organic species can substantially influence DTT consumption.[36] OP^{DTT} could be expressed as a multivariate non-linear function of individual components. Given the wide range of OP_v^{DTT} values reported in the literature, particles heavily influenced by combustion sources were selected for comparison with the present study. The OP_v^{DTT} values obtained in this study approach the higher values reported in the literature for wood and biomass burning particles, which range from approximately 0.33 to 50 nmol min^{-1} m^{-3}.[8,46] All OP_v^{DTT} values for the tested biomass combustion-emitted particles were substantially lower than those reported for trash burning emissions, which range from 98 to 3510 nmol min^{-1} m^{-3}.[97] It is important to note that the differences in sampling strategies, PM concentration levels, and assay protocols may limit the direct quantitative comparisons across studies.

3.4. Association of biomass compositions, particulate emissions, and OP

In this study, the emitted PM_1 mass concentration was observed to be highest for softwood pellets, followed by softwood chips, hardwood chips, and hardwood pellets, respectively. High particle number emissions were measured from each fuel combustion. Metal components in PM_1 emitted from biomass combustion are influenced by the concentrations of ash-forming elements in the fuels and their release during combustion. OC and EC contents are influenced by the completeness of the combustion, where high PM_1 mass concentration observed from softwood combustion consisted majorly of EC content. A summary heatmap was constructed and presented in Table 2 to provide an overview of the analyzed compositions of combustion-emitted particle emissions and their OP.

We have found that biomass fuels associated with high PM mass emissions did not necessarily exhibit high OP, whereas some biomass combustion cases with relatively low PM mass emissions produced PM_1 with elevated OP. This indicates that high OP values are not directly correlated with PM mass emissions alone. Instead, biomass combustion-emitted PM_1 with high intrinsic OP appears to be strongly influenced by particle chemical composition, particularly organic and elemental constituents. In the present study, redox-active transition metals such as Fe, Cu, and Zn, along with elements including Na, P, Mn, Ba, Tl, and the OC fractions, were observed to influence OP_m^{AA}. However, not all elemental influences observed for OP_m^{AA} were reflected in OP_v^{AA}. Notably, the EC fraction showed an influence on OP_v^{AA}, consistent with previous studies reporting strong associations between EC and OP_v^{AA},[36,56] suggesting that OP_v^{AA} may be linked to EC dominance in our PM_1 samples. Exceptionally high PM_1 mass concentrations from certain biomass combustion substantially altered the observed trends

Table 2 Summary heatmap of combustion-emitted particle emissions, their characteristics and OP assessment[a]

Analysis		Unit	Biomass types			
			Hardwood chips	Softwood chips	Hardwood pellets	Softwood pellets
Mass concentration	PM_1	mg m^{-3} (0 °C, 1 atm, 10% O_2, dry gas)	63.52 (9.94)	74.69 (26.38)	17.31 (10.17)	115.51 (29.30)
Number size distribution	Particle number concentration	# m^{-3} (0 °C, 1 atm, 10% O_2, dry gas)	2.85×10^7 (8.05×10^6)	5.25×10^7 (5.33×10^6)	2.35×10^7 (2.32×10^7)	4.85×10^7 (6.51×10^6)
	GMD	μm	0.173 (0.014)	0.123 (0.004)	0.126 (0.002)	0.176 (0.008)
OC/EC of PM_1	OC/TC		0.17	0.15	0.38	0.04
	EC/TC		0.83	0.85	0.62	0.96
	OC/EC		0.21	0.18	0.63	0.04
Elemental compositions of PM_1	Na	μg mg^{-1} of PM_1	11.00	6.47	20.28	4.96
	Mg		0.39	1.13	2.45	0.49
	Al		<LOQ	0.88	2.70	1.45
	P		0.95	0.81	2.99	0.72
	K		65.00	16.44	49.04	18.03
	Zn		1.54	0.69	3.91	1.41
	Ti		<LOQ	0.0631	<LOQ	<LOQ
	Fe		<LOQ	0.1077	0.6028	0.1260
	Cr		<LOQ	0.0084	0.0162	0.0110
	Mn		0.0641	0.0644	0.5285	0.0595
	Co		0.0012	0.0022	<LOQ	0.0002
	Cu		0.0642	0.0322	0.2095	0.0668
	Sr		0.0026	0.0067	0.0198	0.0041
	Mo		0.0038	0.0131	0.0261	0.0046
	Cd		0.0131	0.0061	0.0215	0.0142
	Sn		0.0033	0.0022	0.0208	0.0075
	Sb		0.0037	0.0031	0.0437	0.0121
	Ba		0.0087	0.0138	0.0879	0.0113
	Tl		0.0008	0.0005	0.0022	0.0006
	Pb		0.1019	0.0493	0.3753	0.2985
	Bi		0.0387	0.0176	0.0184	0.0067
	Na	μg m^{-3}	698.63	483.55	351.07	572.90
	Mg		24.66	84.54	42.42	56.33
	Al		<LOQ	65.39	46.75	167.24
	P		60.38	60.54	51.71	82.78
	K		4128.81	1227.84	848.79	2082.23
	Zn		97.72	51.64	67.63	163.36
	Ti		<LOQ	4.72	<LOQ	<LOQ
	Fe		<LOQ	8.04	10.43	14.55
	Cr		<LOQ	0.63	0.28	1.28
	Mn		4.07	4.81	9.15	6.87
	Co		0.08	0.16	<LOQ	0.02
	Cu		4.07	2.41	3.63	7.72
	Sr		0.17	0.50	0.34	0.48
	Mo		0.24	0.98	0.45	0.53
	Cd		0.83	0.45	0.37	1.64
	Sn		0.21	0.16	0.36	0.86
	Sb		0.23	0.23	0.76	1.40
	Ba		0.56	1.03	1.52	1.30
	Tl		0.05	0.04	0.04	0.07
	Pb		6.47	3.68	6.50	34.48
	Bi		2.46	1.32	0.32	0.78
OP of PM_1	OP_m^{AA}	nmol min^{-1} μg^{-1}	0.0086 (0.0023)	0.0059 (0.0023)	0.0176 (0.0085)	0.0051 (0.0014)
	OP_v^{AA}	nmol min^{-1} m^{-3}	544.14 (148.38)	443.32 (170.58)	304.04 (147.79)	583.51 (159.56)
	OP_m^{DTT}	nmol min^{-1} μg^{-1}	0.0005 (0.0002)	0.0003 (0.0002)	0.0040 (0.0019)	0.0002 (0.0001)
	OP_v^{DTT}	nmol min^{-1} m^{-3}	31.38 (15.01)	20.87 (12.24)	68.67 (32.90)	21.30 (14.92)

[a] Particle concentration (mass and number), and OP results are reported as "average (standard deviation)". Elemental compositions of PM_1 reported in concentration (μg m^{-3}) were calculated with PM_1 mass concentration. "<LOQ" is below the limit of ICP-MS quantification (Al 0.20809 μg mg^{-1}, Ti 0.03964 μg mg^{-1}, Fe 0.03624 μg mg^{-1}, Cr 0.00039 μg mg^{-1}, and Co 0.00005 μg mg^{-1}). The color code was used to range from low (green) to high (red) values within each analysis.

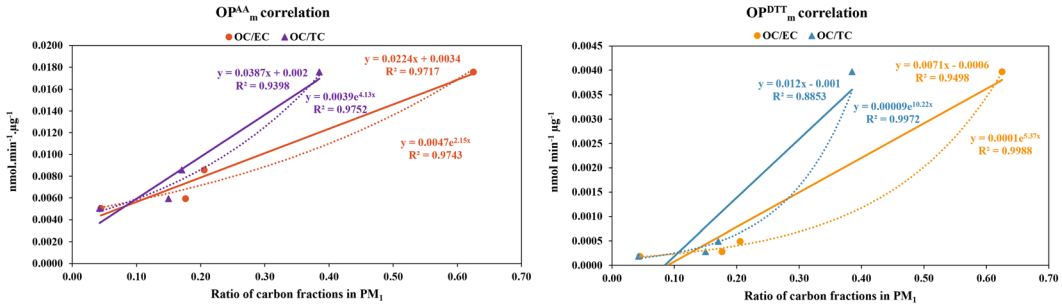

Fig. 9 Correlation of intrinsic OP and OC fractions from combustion-emitted PM_1 of different biomass fuels.

of OP^{AA}. For the DTT assay, contributions from similar components were also observed for OP_m^{DTT}. These elements were also found in other studies to contribute to the assay reaction.[8,88] Nevertheless, the interpretation of OP_v^{DTT} remains challenging due to the non-linear and multivariate interactions between particle components and the DTT assay, particularly those involving metal ions.[31] A recent study also observed differing correlations between PM composition and OP^{DTT} normalized by mass and volume.[98] Accordingly, trends observed in elemental concentrations of emitted-PM did not consistently reflect OP_v^{DTT} behavior, highlighting the non-additive nature of component interactions.

Furthermore, synergistic and antagonistic interactions among PM constituents may occur when considering total particle concentrations in OP assays. Previous studies have reported antagonistic effects arising from metal–organic (*e.g.*, Fe and water-soluble OC) and metal–metal (*e.g.*, Fe and Cu) interactions, which can suppress measured OP responses.[36] Additional parameters, such as the solubility of extracted compounds, may further influence OP measurements. As mentioned in a previous study, the solubility of transition metals determines the influence on OP, as water-soluble metal fractions are more readily mobilized and bioavailable than their water-insoluble fractions, although both may contribute to the overall OP responses.[35] Additionally, atmospheric aging processes can alter particle oxidative properties.[99] Recent research reported that oxidative aging can lead to the production of oxygen-containing functional groups (quinone and epoxide), which increase the OP in the carbon-containing particles.[100–102] These observations underscore the importance of investigating OP in relation to both particle compositions and emission source characteristics.

Since we found that the OC fraction, which belonged to the major part (carbonaceous compounds) of our PM_1 samples, strongly influenced both intrinsic OP metrics (AA and DTT assays), the OC content of primary emitted particles is thus important in inducing oxidative reactions. To further investigate the OC fraction correlation with intrinsic OP, we plotted OP_m^{AA} and OP_m^{DTT} against OC/TC and OC/EC for PM_1 emitted from each biomass combustion and presented in Fig. 9. Two correlations are presented, including linear regression and exponential models. The coefficient of determination (r^2) of OC/EC in linear regression was 0.972 and 0.95 for OP_m^{AA} and OP_m^{DTT}, respectively. In addition, the r^2 values from OP assays and OC/EC for the exponential model were also more than 0.97, indicating an important relationship among the variables in both models. For OC/TC, the data showed a better fit to an exponential model with $r^2 = 0.975$ and $r^2 = 0.997$ for OP_m^{AA} and OP_m^{DTT}, respectively. In accordance with Segakweng *et al.*, a high correlation (0.69) has been reported for the OC ratio of PM_1 and OP_m^{DTT} from outdoor air sampling in urban settlements, suggesting the influence of domestic biomass burning.[98] It is worth mentioning that further biomass combustion parameters, including alternative biomass types and combustion appliances, are important to be investigated and analyzed. Given the limited sample size in this study, the observed relationships may limit the representativeness of the inferred trends. Future studies would benefit from a larger dataset encompassing a wider range of biomass types, combustion technologies, and operating conditions. This would enable robust statistical analyses, which may facilitate future modeling approaches for calculating and predicting both intrinsic OP and volume-normalized OP relationships with particle composition-related drivers, leading to an enhancement in the regulatory framework for biomass combustion emissions.

4 Conclusion

This study presents the OP of PM_1 emitted from biomass combustion. The associations between biomass and PM_1 characteristics with OP results were also investigated. Although the tested biomass samples complied with established chemical composition standards, they demonstrated distinct emission characteristics and varied potential impacts. In our case, biomass samples with the highest PM mass concentrations did not consistently exhibit the highest OP values. Our softwood pellets emitted a substantial number of particles. However, the intrinsic OP was found to be lower than that of hardwood pellets, which contained significant OC fractions and inorganic elements. This suggests that chemical compositions of combustion-emitted PM_1, notably organic components, can significantly influence their OP and potential impacts. A thorough PM assessment should be incorporated into fuel selection protocols for biomass combustion. Additionally, we found a strong correlation between the OC fraction of carbonaceous compounds and the intrinsic OP. In linear regression, OC/EC strongly correlated with OP_m^{AA}, and OP_m^{DTT} demonstrated an r^2 of approximately 0.95. OC/EC can be a beneficial parameter in

investigating the intrinsic OP of primary particles emitted from biomass combustion. A potential prediction model could be developed to facilitate the assessment of combustion-emitted particles. We have also observed different trends from volume-normalized OP^{AA} and OP^{DTT}. Since AA and DTT assays target different components, particle–assay interactions may lead to differing OP responses. Applying both OP assays to assess the emissions of biomass combustion is found to give prominent information to capture the different emission compositions. Based on the findings of this study, the differing trends observed between assays and normalization approaches reflect the multi-dimensional behavior of OP, which depends on particle compositions and assay sensitivities. Our results highlight the need for standardization and harmonization of PM sampling procedures and OP assessment methodologies to ensure comparability across studies. Moreover, OP metrics derived from acellular assays such as AA and DTT provide complementary but not necessarily equivalent information, as they undergo different redox-active particle components and may not directly reflect biological responses. To support informed biomass selection, future studies should integrate OP measurements with cellular-based toxicological assessments to validate the relevance of OP indicators to health outcomes. Given the complex relationships among biomass composition, combustion-emitted particles, and their physicochemical properties, an integrative framework that combines chemical composition, OP assays, and health-impact indicators will be necessary. Such an approach would enable more robust evaluation of fuel choices, support the development of improved emission control strategies, and contribute to minimizing adverse health effects associated with residential biomass combustion.

Author contributions

Marie Khedari: writing – original draft, conceptualization, methodology, investigation, formal analysis, visualization. Audrey Villot: writing – review & editing, investigation, project administration, resources, funding acquisition, supervision. Joulanda Taha: investigation (oxidative potential assessment), Olli Sippula: writing – review & editing, investigation, project administration, resources, supervision. Pasi Jalava: writing – review & editing, investigation, project administration, resources, funding acquisition, supervision. Yves Andres: writing – review & editing, investigation, project administration, resources, funding acquisition, supervision.

Conflicts of interest

There are no conflicts to declare.

Abbreviations

AA	Ascorbic acid
AC	Ash content
ADEME	Agence de la Transition Écologique (The French agency for ecological transition)
ARDS	Acute respiratory distress syndrome
BEI	Backscattered electron imaging
COPD	Chronic obstructive pulmonary disease
DTNB	5,5′-Dithiobis-(2-nitrobenzoic acid)
DTT	Dithiothreitol
EC	Elemental carbon
EDX	Energy-dispersive X-ray spectroscopy
ELPI	Electrical low pressure impactor
FC	Fixed carbon
GMD	Geometric particle number mean diameter
ICP-MS	Inductively coupled plasma mass spectrometer
OC	Organic carbon
OM	Organic matter
OP	Oxidative potential
MC	Moisture content
PAHs	Polycyclic aromatic hydrocarbons
PM	Particulate matter
ROS	Reactive oxygen species
SEI	Secondary electron imaging
SEM	Scanning electron microscope
TGA	Thermogravimetric analysis
VM	Volatile matter

Data availability

The supporting data has been provided as part of the supplementary information (SI). Supplementary information: Tables S1–S5. Fig. S1–S3. See DOI: https://doi.org/10.1039/d5ea00177c.

Acknowledgements

This research was supported by IMT Atlantique (Department of Energy Systems and Environment, Nantes, France) and the University of Eastern Finland (Department of Environmental and Biological Sciences, Kuopio, Finland). This study was supported by Research council of Finland decision number 362436, Role of oxidation and Nrf2 in systematic approach to study adverse effects of ultrafine particles. The SEM-EDX measurement was performed using the IMN's characterization platform, PLASSMAT, Nantes, France. The ICP-MS experiment was performed by Hanna Koponen at Fine Particle and Aerosol Technology Laboratory, UEF, Kuopio, Finland.

References

1 P. I. Jalava, M. S. Happo, J. Kelz, T. Brunner, P. Hakulinen, J. Mäki-Paakkanen, A. Hukkanen, J. Jokiniemi, I. Obernberger and M.-R. Hirvonen, In vitro toxicological characterization of particulate emissions from residential biomass heating systems based on old and new technologies, *Atmos. Environ.*, 2012, **50**, 24–35.
2 K. Jiang, R. Xing, Z. Luo, W. Huang, F. Yi, Y. Men, N. Zhao, Z. Chang, J. Zhao, B. Pan and G. Shen, Pollutant emissions from biomass burning: A review on emission

characteristics, environmental impacts, and research perspectives, *Particuology*, 2024, **85**, 296–309.
3 L. P. Naeher, M. Brauer, M. Lipsett, J. T. Zelikoff, C. D. Simpson, J. Q. Koenig and K. R. Smith, Woodsmoke Health Effects: A Review, *Inhalation Toxicol.*, 2007, **19**, 67–106.
4 M. Khedari, A. Villot, O. Sippula, P. Jalava and Y. Andres, A comprehensive bibliometric analysis of research on health and environmental impacts of particle emissions from wood combustion in residential heating, *Environ. Sci. Pollut. Res.*, 2025, **32**, 17897–17915.
5 Z. Fang, A. Lai, D. Cai, C. Li, R. Carmieli, J. Chen, X. Wang and Y. Rudich, Secondary Organic Aerosol Generated from Biomass Burning Emitted Phenolic Compounds: Oxidative Potential, Reactive Oxygen Species, and Cytotoxicity, *Environ. Sci. Technol.*, 2024, **58**, 8194–8206.
6 B. H. Isenor, J. P. Downey, S. A. Whidden, M. M. Fitzgerald and J. P. S. Wong, Oxidative potential of fine particulate matter emitted from traditional and improved biomass cookstoves, *Environ. Sci.: Atmos.*, 2024, **4**, 202–213.
7 O. P. Kurmi, C. Dunster, J. G. Ayres and F. J. Kelly, Oxidative potential of smoke from burning wood and mixed biomass fuels, *Free Radical Res.*, 2013, **47**, 829–835.
8 M. C. Pietrogrande, I. Bertoli, G. Clauser, C. Dalpiaz, R. Dell'Anna, P. Lazzeri, W. Lenzi and M. Russo, Chemical composition and oxidative potential of atmospheric particles heavily impacted by residential wood burning in the alpine region of northern Italy, *Atmos. Environ.*, 2021, **253**, 118360.
9 M. Rinaldi, F. Manarini, M. Lucertini, M. Rapuano, S. Decesari, M. Paglione, M. C. Facchini, C. Lin, D. Ceburnis, C. D. O'Dowd, P. Buckley, S. Hellebust, J. Wenger and J. Ovadnevaite, Important Contribution to Aerosol Oxidative Potential from Residential Solid Fuel Burning in Central Ireland, *Atmosphere*, 2024, **15**, 436.
10 S. Yadav and H. C. Phuleria, in *Measurement, Analysis and Remediation of Environmental Pollutants*, ed. T. Gupta, S. P. Singh, P. Rajput and A. K. Agarwal, Springer Singapore, Singapore, 2020, pp. 333–356.
11 P. Shahpoury, Z. W. Zhang, A. Filippi, S. Hildmann, S. Lelieveld, B. Mashtakov, B. R. Patel, A. Traub, D. Umbrio, M. Wietzoreck, J. Wilson, T. Berkemeier, V. Celo, E. Dabek-Zlotorzynska, G. Evans, T. Harner, K. Kerman, G. Lammel, M. Noroozifar, U. Pöschl and H. Tong, Inter-comparison of oxidative potential metrics for airborne particles identifies differences between acellular chemical assays, *Atmos. Pollut. Res.*, 2022, **13**, 101596.
12 J. Choi, J. Y. Oh, Y. S. Lee, K. H. Min, G. Y. Hur, S. Y. Lee, K. H. Kang and J. J. Shim, Harmful impact of air pollution on severe acute exacerbation of chronic obstructive pulmonary disease: particulate matter is hazardous, *COPD*, 2018, **13**, 1053–1059.
13 Z. Leni, L. Künzi and M. Geiser, Air pollution causing oxidative stress, *Curr. Opin. Toxicol.*, 2020, **20–21**, 1–8.
14 C. C. Lim and G. D. Thurston, Air Pollution, Oxidative Stress, and Diabetes: a Life Course Epidemiologic Perspective, *Curr. Diabetes Rep.*, 2019, **19**, 58.
15 G. Pizzino, N. Irrera, M. Cucinotta, G. Pallio, F. Mannino, V. Arcoraci, F. Squadrito, D. Altavilla and A. Bitto, Oxidative Stress: Harms and Benefits for Human Health, *Oxid. Med. Cell. Longevity*, 2017, **2017**, 8416763.
16 Y. Taniyama and K. K. Griendling, Reactive Oxygen Species in the Vasculature: Molecular and Cellular Mechanisms, *Hypertension*, 2003, **42**, 1075–1081.
17 H. Sies, Oxidative stress: oxidants and antioxidants, *Exp. Physiol.*, 1997, **82**, 291–295.
18 N. K. Binsaleh, R. Eltayeb, H. Qanash, M. A. Aziz, R. Albaradie and M. W. A. Khan, Presence of Circulatory Autoantibodies Against ROS-Modified Histone H1 Protein in Lymphoma Patients, *Front. Genet.*, 2022, **13**, 909903.
19 N. Li, M. Hao, R. F. Phalen, W. C. Hinds and A. E. Nel, Particulate air pollutants and asthma, *Clin. Immunol.*, 2003, **109**, 250–265.
20 Q. Rahman, P. Abidi, F. Afaq, D. Schiffmann, B. T. Mossman, D. W. Kamp and M. Athar, Glutathione Redox System in Oxidative Lung Injury, *Crit. Rev. Toxicol.*, 1999, **29**, 543–568.
21 The European Commission, Directive (EU) 2024/2881 of the European Parliament and of the Council of 23 October 2024 on ambient air quality and cleaner air for Europe (recast), https://eur-lex.europa.eu/eli/dir/2024/2881/oj, (accessed 8 November 2025).
22 L. J. Borlaza, S. Weber, A. Marsal, G. Uzu, V. Jacob, J.-L. Besombes, M. Chatain, S. Conil and J.-L. Jaffrezo, Nine-year trends of PM10 sources and oxidative potential in a rural background site in France, *Atmos. Chem. Phys.*, 2022, **22**, 8701–8723.
23 C. Molina, C. A. Manzano, R. Toro A. and M. A. Leiva G, The oxidative potential of airborne particulate matter in two urban areas of Chile: More than meets the eye, *Environ. Int.*, 2023, **173**, 107866.
24 A. Bergomi, E. Carrara, E. Festa, C. Colombi, E. Cuccia, B. Biffi, V. Comite and P. Fermo, Optimization and Application of Analytical Assays for the Determination of Oxidative Potential of Outdoor and Indoor Particulate Matter, *Atmosphere*, 2024, **15**, 772.
25 S. S. Khurshid, S. Emmerich and A. Persily, Oxidative potential of particles at a research house: Influencing factors and comparison with outdoor particles, *Build. Environ.*, 2019, **163**, 106275.
26 G. Melzi, L. Massimi, M. A. Frezzini, M. Iulini, N. Tarallo, M. Rinaldi, M. Paglione, E. Nozza, F. Crova, S. Valentini, G. Valli, F. Costabile, S. Canepari, S. Decesari, R. Vecchi, M. Marinovich and E. Corsini, Redox-activity and in vitro effects of regional atmospheric aerosol pollution: Seasonal differences and correlation between oxidative potential and in vitro toxicity of PM1, *Toxicol. Appl. Pharmacol.*, 2024, **485**, 116913.
27 F. Hedayat, S. Stevanovic, B. Miljevic, S. Bottle and Z. D. Ristovski, Review-evaluating the molecular assays for

measuring the oxidative potential of particulate matter, *Chem. Ind. Chem. Eng. Q.*, 2015, **21**, 201–210.
28 J. G. Ayres, P. Borm, F. R. Cassee, V. Castranova, K. Donaldson, A. Ghio, R. M. Harrison, R. Hider, F. Kelly, I. M. Kooter, F. Marano, R. L. Maynard, I. Mudway, A. Nel, C. Sioutas, S. Smith, A. Baeza-Squiban, A. Cho, S. Duggan and J. Froines, Evaluating the Toxicity of Airborne Particulate Matter and Nanoparticles by Measuring Oxidative Stress Potential—A Workshop Report and Consensus Statement, *Inhalation Toxicol.*, 2008, **20**, 75–99.
29 H. Sekine, H. Ito and Y. Sekine, Effect of Werner-Type Complex Formation of Cu2+ and Fe2+ on Oxidative Potentials Assessed Using Ascorbic Acid Assay, *Atmosphere*, 2025, **16**, 192.
30 J. Shen, P. T. Griffiths, S. J. Campbell, B. Utinger, M. Kalberer and S. E. Paulson, Ascorbate oxidation by iron, copper and reactive oxygen species: review, model development, and derivation of key rate constants, *Sci. Rep.*, 2021, **11**, 7417.
31 M. Visentin, A. Pagnoni, E. Sarti and M. C. Pietrogrande, Urban PM2.5 oxidative potential: Importance of chemical species and comparison of two spectrophotometric cell-free assays, *Environ. Pollut.*, 2016, **219**, 72–79.
32 J. G. Charrier and C. Anastasio, On dithiothreitol (DTT) as a measure of oxidative potential for ambient particles: evidence for the importance of soluble transition metals, *Atmos. Chem. Phys.*, 2012, **12**, 9321–9333.
33 A. K. Cho, C. Sioutas, A. H. Miguel, Y. Kumagai, D. A. Schmitz, M. Singh, A. Eiguren-Fernandez and J. R. Froines, Redox activity of airborne particulate matter at different sites in the Los Angeles Basin, *Environ. Res.*, 2005, **99**, 40–47.
34 H. Jiang, C. M. S. Ahmed, Z. Zhao, J. Y. Chen, H. Zhang, A. Canchola and Y.-H. Lin, Role of functional groups in reaction kinetics of dithiothreitol with secondary organic aerosols, *Environ. Pollut.*, 2020, **263**, 114402.
35 D. Gao, S. Ripley, S. Weichenthal and K. J. Godri Pollitt, Ambient particulate matter oxidative potential: Chemical determinants, associated health effects, and strategies for risk management, *Free Radicals Biol. Med.*, 2020, **151**, 7–25.
36 D. Gao, K. J. Godri Pollitt, J. A. Mulholland, A. G. Russell and R. J. Weber, Characterization and comparison of PM2.5 oxidative potential assessed by two acellular assays, *Atmos. Chem. Phys.*, 2020, **20**, 5197–5210.
37 F. Fachinger, F. Drewnick, R. Gieré and S. Borrmann, How the user can influence particulate emissions from residential wood and pellet stoves: Emission factors for different fuels and burning conditions, *Atmos. Environ.*, 2017, **158**, 216–226.
38 H. Rinta-Kiikka, K. Dahal, J. Louhisalmi, H. Koponen, O. Sippula, K. Krpec and J. Tissari, The Effect of Wood Species on Fine Particle and Gaseous Emissions from a Modern Wood Stove, *Atmosphere*, 2024, **15**, 839.
39 The European Commission, Commission Regulation (EU) 2015/1189 of 28 April 2015 implementing Directive 2009/125/EC of the European Parliament and of the Council with regard to ecodesign requirements for solid fuel boilers, https://eur-lex.europa.eu/eli/reg/2015/1189/2017-01-09/eng, accessed 10 July 2025.
40 K. Křůmal, P. Mikuška, J. Horák, F. Hopan and K. Krpec, Comparison of emissions of gaseous and particulate pollutants from the combustion of biomass and coal in modern and old-type boilers used for residential heating in the Czech Republic, Central Europe, *Chemosphere*, 2019, **229**, 51–59.
41 T. Salthammer, T. Schripp, S. Wientzek and M. Wensing, Impact of operating wood-burning fireplace ovens on indoor air quality, *Chemosphere*, 2014, **103**, 205–211.
42 P. Krecl, E. Hedberg Larsson, J. Ström and C. Johansson, Contribution of residential wood combustion and other sources to hourly winter aerosol in Northern Sweden determined by positive matrix factorization, *Atmos. Chem. Phys.*, 2008, **8**, 3639–3653.
43 D. E. Schraufnagel, The health effects of ultrafine particles, *Exp. Mol. Med.*, 2020, **52**, 311–317.
44 Y. Hu, M. Wu, Y. Li and X. Liu, Influence of PM1 exposure on total and cause-specific respiratory diseases: a systematic review and meta-analysis, *Environ. Sci. Pollut. Res.*, 2022, **29**, 15117–15126.
45 M. C. Pietrogrande, M. R. Perrone, F. Manarini, S. Romano, R. Udisti and S. Becagli, PM10 oxidative potential at a Central Mediterranean Site: Association with chemical composition and meteorological parameters, *Atmos. Environ.*, 2018, **188**, 97–111.
46 S. Yadav, T. S. Kapoor, P. Vernekar and H. C. Phuleria, Examining the Chemical and Optical Properties of Biomass-burning Aerosols and their Impact on Oxidative Potential, *Aerosol Air Qual. Res.*, 2023, **23**, 230102.
47 L. Shao, C. Hou, C. Geng, J. Liu, Y. Hu, J. Wang, T. Jones, C. Zhao and K. BéruBé, The oxidative potential of PM 10 from coal, briquettes and wood charcoal burnt in an experimental domestic stove, *Atmos. Environ.*, 2016, **127**, 372–381.
48 P. Toulmin, A. K. Baird, B. C. Clark, K. Keil and H. J. Rose, Inorganic chemical investigation by x-ray fluorescence analysis: The Viking Mars Lander, *Icarus*, 1973, **20**, 153–178.
49 T. Emiola-Sadiq, L. Zhang and A. K. Dalai, Thermal and Kinetic Studies on Biomass Degradation *via* Thermogravimetric Analysis: A Combination of Model-Fitting and Model-Free Approach, *ACS Omega*, 2021, **6**, 22233–22247.
50 H. H. Muigai, B. J. Choudhury, P. Kalita and V. S. Moholkar, Co–pyrolysis of biomass blends: Characterization, kinetic and thermodynamic analysis, *Biomass Bioenergy*, 2020, **143**, 105839.
51 ADEME, Validation of a common European method for determining particulate emissions from domestic solid-fuel heating appliances (In French), https://librairie.ademe.fr/energies-renouvelables-reseaux-et-stockage/3780-validation-d-une-methode-commune-au-niveau-europeen-de-determination-des-emissions-de-particules-des-appareils-de-chauffage-domestique-a-combustibles-solides.html, accessed 1 February 2024.

52 A. Järvinen, M. Aitomaa, A. Rostedt, J. Keskinen and J. Yli-Ojanperä, Calibration of the new electrical low pressure impactor (ELPI+), *J. Aerosol Sci.*, 2014, **69**, 150–159.
53 M. R. Perrone, I. Bertoli, S. Romano, M. Russo, G. Rispoli and M. C. Pietrogrande, PM2.5 and PM10 oxidative potential at a Central Mediterranean Site: Contrasts between dithiothreitol- and ascorbic acid-measured values in relation with particle size and chemical composition, *Atmos. Environ.*, 2019, **210**, 143–155.
54 M. C. Pietrogrande, C. Dalpiaz, R. Dell'Anna, P. Lazzeri, F. Manarini, M. Visentin and G. Tonidandel, Chemical composition and oxidative potential of atmospheric coarse particles at an industrial and urban background site in the alpine region of northern Italy, *Atmos. Environ.*, 2018, **191**, 340–350.
55 D. Gao, T. Fang, V. Verma, L. Zeng and R. J. Weber, A method for measuring total aerosol oxidative potential (OP) with the dithiothreitol (DTT) assay and comparisons between an urban and roadside site of water-soluble and total OP, *Atmos. Meas. Tech.*, 2017, **10**, 2821–2835.
56 A. Yang, A. Jedynska, B. Hellack, I. Kooter, G. Hoek, B. Brunekreef, T. A. J. Kuhlbusch, F. R. Cassee and N. A. H. Janssen, Measurement of the oxidative potential of PM2.5 and its constituents: The effect of extraction solvent and filter type, *Atmos. Environ.*, 2014, **83**, 35–42.
57 S. Kasurinen, P. I. Jalava, O. Uski, M. S. Happo, T. Brunner, J. Mäki-Paakkanen, J. Jokiniemi, I. Obernberger and M.-R. Hirvonen, Toxicological characterization of particulate emissions from straw, *Miscanthus* , and poplar pellet combustion in residential boilers, *Aerosol Sci. Technol.*, 2016, **50**, 41–51.
58 C. Roper, L. S. Delgado, D. Barrett, S. L. Massey Simonich and R. L. Tanguay, $PM_{2.5}$ Filter Extraction Methods: Implications for Chemical and Toxicological Analyses, *Environ. Sci. Technol.*, 2019, **53**, 434–442.
59 M. Mancini, G. Toscano, G. Feliciangeli, E. Leoni and D. Duca, Investigation on woodchip quality with respect to ISO standards and relationship among quality parameters, *Fuel*, 2020, **279**, 118559.
60 D. Dalkhsuren, K. Iwabuchi, T. Itoh, T. Narita, M. I. Piash, B. Nachin and G. Sukhbaatar, Effects of Ash Composition and Combustion Temperature on Reduced Particulate Matter Emission by Biomass Carbonization, *Bioenergy Res.*, 2023, **16**, 1629–1638.
61 O. Sippula, H. Lamberg, J. Leskinen, J. Tissari and J. Jokiniemi, Emissions and ash behavior in a 500 kW pellet boiler operated with various blends of woody biomass and peat, *Fuel*, 2017, **202**, 144–153.
62 W. Yang, D. Pudasainee, R. Gupta, W. Li, B. Wang and L. Sun, An overview of inorganic particulate matter emission from coal/biomass/MSW combustion: Sampling and measurement, formation, distribution, inorganic composition and influencing factors, *Fuel Process. Technol.*, 2021, **213**, 106657.
63 O. Sippula, J. Hokkinen, H. Puustinen, P. Yli-Pirilä and J. Jokiniemi, Particle Emissions from Small Wood-fired District Heating Units, *Energy Fuels*, 2009, **23**, 2974–2982.
64 European Pellet Council, 2015.
65 B. Meryemoglu, B. Kaya Ozsel and S. Irmak, Evaluation of hardwood or softwood bark biomass as feed materials for aqueous-phase reforming gasification process, *Int. J. Hydrogen Energy*, 2024, **53**, 1044–1051.
66 M. Raud, T. Kikas, O. Sippula and N. J. Shurpali, Potentials and challenges in lignocellulosic biofuel production technology, *Renewable Sustainable Energy Rev.*, 2019, **111**, 44–56.
67 O. Sippula, K. Hytönen, J. Tissari, T. Raunemaa and J. Jokiniemi, Effect of Wood Fuel on the Emissions from a Top-Feed Pellet Stove, *Energy Fuels*, 2007, **21**, 1151–1160.
68 J. Tissari, O. Sippula, J. Kouki, K. Vuorio and J. Jokiniemi, Fine Particle and Gas Emissions from the Combustion of Agricultural Fuels Fired in a 20 kW Burner, *Energy Fuels*, 2008, **22**, 2033–2042.
69 L. Tumolva, J.-Y. Park, J. Kim, A. L. Miller, J. C. Chow, J. G. Watson and K. Park, Morphological and Elemental Classification of Freshly Emitted Soot Particles and Atmospheric Ultrafine Particles using the TEM/EDS, *Aerosol Sci. Technol.*, 2010, **44**, 202–215.
70 F. Usman, B. Zeb, K. Alam, Z. Huang, A. Shah, I. Ahmad and S. Ullah, In-Depth Analysis of Physicochemical Properties of Particulate Matter (PM10, PM2.5 and PM1) and Its Characterization through FTIR, XRD and SEM–EDX Techniques in the Foothills of the Hindu Kush Region of Northern Pakistan, *Atmosphere*, 2022, **13**, 124.
71 S. Guofeng, W. Siye, W. Wen, Z. Yanyan, M. Yujia, W. Bin, W. Rong, L. Wei, S. Huizhong, H. Ye, Y. Yifeng, W. Wei, W. Xilong, W. Xuejun and T. Shu, Emission Factors, Size Distributions, and Emission Inventories of Carbonaceous Particulate Matter from Residential Wood Combustion in Rural China, *Environ. Sci. Technol.*, 2012, **46**, 4207–4214.
72 R. Nyström, R. Lindgren, R. Avagyan, R. Westerholm, S. Lundstedt and C. Boman, Influence of Wood Species and Burning Conditions on Particle Emission Characteristics in a Residential Wood Stove, *Energy Fuels*, 2017, **31**, 5514–5524.
73 M. Cui, Y. Xu, B. Yu, C. Yan, J. Li, M. Zheng and Y. Chen, Characterization of carbonaceous matter emitted from residential coal and biomass combustion by experimental simulation, *Atmos. Environ.*, 2023, **293**, 119447.
74 Y.-N. Wang, Y. Cheng, Z.-L. Gu, J.-T. Yang and H.-H. Ren, Emission Factors and Inventories of Carbonaceous Aerosols from Residential Biomass Burning in Guizhou Province, China, *Atmosphere*, 2022, **13**, 1595.
75 H. Lamberg, J. Tissari, J. Jokiniemi and O. Sippula, Fine Particle and Gaseous Emissions from a Small-Scale Boiler Fueled by Pellets of Various Raw Materials, *Energy Fuels*, 2013, **27**, 7044–7053.
76 E. D. Vicente and C. A. Alves, An overview of particulate emissions from residential biomass combustion, *Atmos. Res.*, 2018, **199**, 159–185.
77 E. D. Vicente, M. A. Duarte, A. I. Calvo, T. F. Nunes, L. A. C. Tarelho, D. Custódio, C. Colombi, V. Gianelle, A. Sanchez De La Campa and C. A. Alves, Influence of operating conditions on chemical composition of

particulate matter emissions from residential combustion, *Atmos. Res.*, 2015, **166**, 92–100.

78 J. Leskinen, J. Tissari, O. Uski, A. Virén, T. Torvela, T. Kaivosoja, H. Lamberg, I. Nuutinen, T. Kettunen, J. Joutsensaari, P. I. Jalava, O. Sippula, M.-R. Hirvonen and J. Jokiniemi, Fine particle emissions in three different combustion conditions of a wood chip-fired appliance – Particulate physico-chemical properties and induced cell death, *Atmos. Environ.*, 2014, **86**, 129–139.

79 A. Mukherjee, A. Hartikainen, M. Somero, V. Luostari, M. Ihalainen, C. P. Rüger, T. Kekäläinen, V. H. Nissinen, L. M. F. Barreira, H. Koponen, T. Kokkola, D. Li, L. Vettikkat, P. Yli-Pirilä, M. Shahzaib, M. M. Ruppel, V. Vakkari, K. Jaars, S. J. Siebert, A. Buchholz, K. Köster, P. G. Van Zyl, H. Timonen, N. Kinnunen, J. Jänis, A. Virtanen, A. Virkkula and O. Sippula, Brown carbon emissions from laboratory combustion of Eurasian arctic-boreal and South African savanna biomass, *Atmos. Chem. Phys.*, 2025, **25**, 16747–16774.

80 R. Saleh, Z. Cheng and K. Atwi, The Brown–Black Continuum of Light-Absorbing Combustion Aerosols, *Environ. Sci. Technol. Lett.*, 2018, **5**, 508–513.

81 H. Suhonen, A. Laitinen, M. Kortelainen, H. Koponen, N. Kinnunen, M. Suvanto, J. Tissari and O. Sippula, Novel fine particle reduction method for wood stoves based on high-temperature electric collection of naturally charged soot particles, *J. Cleaner Prod.*, 2021, **312**, 127831.

82 A. Hartikainen, P. Tiitta, M. Ihalainen, P. Yli-Pirilä, J. Orasche, H. Czech, M. Kortelainen, H. Lamberg, H. Suhonen, H. Koponen, L. Hao, R. Zimmermann, J. Jokiniemi, J. Tissari and O. Sippula, Photochemical transformation of residential wood combustion emissions: dependence of organic aerosol composition on OH exposure, *Atmos. Chem. Phys.*, 2020, **20**, 6357–6378.

83 A. Yazdani, N. Dudani, S. Takahama, A. Bertrand, A. S. H. Prévôt, I. El Haddad and A. M. Dillner, Characterization of primary and aged wood burning and coal combustion organic aerosols in an environmental chamber and its implications for atmospheric aerosols, *Atmos. Chem. Phys.*, 2021, **21**, 10273–10293.

84 H. Czech, T. Miersch, J. Orasche, G. Abbaszade, O. Sippula, J. Tissari, B. Michalke, J. Schnelle-Kreis, T. Streibel, J. Jokiniemi and R. Zimmermann, Chemical composition and speciation of particulate organic matter from modern residential small-scale wood combustion appliances, *Sci. Total Environ.*, 2018, **612**, 636–648.

85 J. Noda, R. Bergström, X. Kong, T. L. Gustafsson, B. Kovacevik, M. Svane and J. B. C. Pettersson, Aerosol from Biomass Combustion in Northern Europe: Influence of Meteorological Conditions and Air Mass History, *Atmosphere*, 2019, **10**, 789.

86 J. G. Watson, J. C. Chow and J. E. Houck, PM2.5 chemical source profiles for vehicle exhaust, vegetative burning, geological material, and coal burning in Northwestern Colorado during 1995, *Chemosphere*, 2001, **43**, 1141–1151.

87 O. Sippula, T. Lind and J. Jokiniemi, Effects of chlorine and sulphur on particle formation in wood combustion performed in a laboratory scale reactor, *Fuel*, 2008, **87**, 2425–2436.

88 C. Alves, E. D. Vicente, T. Nunes, Y. Cipoli, I. Charres, E. Yubero, N. Galindo, J. Ryšavý and A. Leitão, Elemental and carbonaceous composition of PM10 and its oxidative potential in schools in Luanda, *Atmos. Environ.*, 2026, **364**, 121640.

89 L. Moufarrej, D. Courcot and F. Ledoux, Assessment of the PM2.5 oxidative potential in a coastal industrial city in Northern France: Relationships with chemical composition, local emissions and long range sources, *Sci. Total Environ.*, 2020, **748**, 141448.

90 M. C. Pietrogrande, I. Bertoli, F. Manarini and M. Russo, Ascorbate assay as a measure of oxidative potential for ambient particles: Evidence for the importance of cell-free surrogate lung fluid composition, *Atmos. Environ.*, 2019, **211**, 103–112.

91 K. R. Daellenbach, G. Uzu, J. Jiang, L.-E. Cassagnes, Z. Leni, A. Vlachou, G. Stefenelli, F. Canonaco, S. Weber, A. Segers, J. J. P. Kuenen, M. Schaap, O. Favez, A. Albinet, S. Aksoyoglu, J. Dommen, U. Baltensperger, M. Geiser, I. El Haddad, J.-L. Jaffrezo and A. S. H. Prévôt, Sources of particulate-matter air pollution and its oxidative potential in Europe, *Nature*, 2020, **587**, 414–419.

92 S. Weber, G. Uzu, A. Calas, F. Chevrier, J.-L. Besombes, A. Charron, D. Salameh, I. Ježek, G. Močnik and J.-L. Jaffrezo, An apportionment method for the oxidative potential of atmospheric particulate matter sources: application to a one-year study in Chamonix, France, *Atmos. Chem. Phys.*, 2018, **18**, 9617–9629.

93 J. G. Charrier and C. Anastasio, Rates of Hydroxyl Radical Production from Transition Metals and Quinones in a Surrogate Lung Fluid, *Environ. Sci. Technol.*, 2015, **49**, 9317–9325.

94 V. Verma, T. Fang, L. Xu, R. E. Peltier, A. G. Russell, N. L. Ng and R. J. Weber, Organic Aerosols Associated with the Generation of Reactive Oxygen Species (ROS) by Water-Soluble $PM_{2.5}$, *Environ. Sci. Technol.*, 2015, **49**, 4646–4656.

95 M. Pirhadi, A. Mousavi, S. Taghvaee, M. M. Shafer and C. Sioutas, Semi-volatile components of PM2.5 in an urban environment: Volatility profiles and associated oxidative potential, *Atmos. Environ.*, 2020, **223**, 117197.

96 Q. Li, A. Wyatt and R. M. Kamens, Oxidant generation and toxicity enhancement of aged-diesel exhaust, *Atmos. Environ.*, 2009, **43**, 1037–1042.

97 H. Vreeland, J. J. Schauer, A. G. Russell, J. D. Marshall, A. Fushimi, G. Jain, K. Sethuraman, V. Verma, S. N. Tripathi and M. H. Bergin, Chemical characterization and toxicity of particulate matter emissions from roadside trash combustion in urban India, *Atmos. Environ.*, 2016, **147**, 22–30.

98 C. K. Segakweng, P. G. Van Zyl, C. Liousse, S. Gnamien, E. Gardrat, J. P. Beukes, K. Jaars, C. Dumat, B. Guinot, M. Josipovic, B. Language, R. P. Burger, S. J. Piketh and T. Xiong, Oxidative potential of atmospheric particulate matter collected in low-income urban settlements in South Africa, *Environ. Sci.: Atmos.*, 2025, **5**, 48–66.

99 J. P. S. Wong, M. Tsagkaraki, I. Tsiodra, N. Mihalopoulos, K. Violaki, M. Kanakidou, J. Sciare, A. Nenes and R. J. Weber, Effects of Atmospheric Processing on the Oxidative Potential of Biomass Burning Organic Aerosols, *Environ. Sci. Technol.*, 2019, **53**, 6747–6756.

100 Q. Li, J. Shang, J. Liu, W. Xu, X. Feng, R. Li and T. Zhu, Physicochemical characteristics, oxidative capacities and cytotoxicities of sulfate-coated, 1,4-NQ-coated and ozone-aged black carbon particles, *Atmos. Res.*, 2015, **153**, 535–542.

101 J. Zhu, Y. Chen, J. Shang, Y. Kuang and T. Zhu, Dithiothreitol (DTT) activity of different fractions of fresh and ozonised soot and quantitative contributions of ozonised products of phenanthrene, *Atmos. Environ.*, 2019, **214**, 116835.

102 Y. Liu and C. K. Chan, The oxidative potential of fresh and aged elemental carbon-containing airborne particles: a review, *Environ. Sci.: Processes Impacts*, 2022, **24**, 525–546.